



Published in final edited form as:

Eur J Radiol. 2009 May ; 70(2): 265–273. doi:10.1016/j.ejrad.2009.01.043.

Imaging Oncogene Expression

Archana Mukherjee, Ph.D,

Postdoctoral Research Fellow, Department of Radiology, Thomas Jefferson University, 361 JAH, 1020, Locust Street, Philadelphia, PA 19107, USA, Email: Archana.Mukherjee@jefferson.edu, Tel: 215-503-7879, Fax: 215-923-9245

Eric Wickstrom, Ph.D, and

Department of Biochemistry and Molecular Biology, Thomas Jefferson University, 233S, 10th street, Suite 219 Philadelphia, PA 19107, USA, Email: eric@tesla.jci.tju.edu, Tel: 215-955-4578, Fax: 215-955-4580

Mathew L. Thakur, Ph.D

Director, Laboratories of Radiopharmaceutical Research and Molecular Imaging, Department of Radiology, Thomas Jefferson University, Kimmel Cancer Centre. Suite 359 JAH, 1020, Locust Street, Philadelphia, PA 19107, USA, Email: Mathew.Thakur@jefferson.edu, Tel: 215-503-7874, Fax: 215-923-9245

Abstract

This review briefly outlines the importance of molecular imaging, particularly imaging of endogenous gene expression for noninvasive genetic analysis of radiographic masses. The concept of antisense imaging agents and the advantages and challenges in the development of hybridization probes for in vivo imaging are described. An overview of the investigations on oncogene expression imaging is given. Finally, the need for further improvement in antisense-based imaging agents and directions to improve oncogene mRNA targeting is stated.

Keywords

Antisense; Imaging; Peptide nucleic acid (PNA); Peptide-PNA conjugates; Positron emission tomography (PET)

1. Introduction

Early diagnosis of cancer remains challenging. Investigational approaches are increasingly focused on development of specific probes that take advantage of the targets that are uniquely expressed or markedly over expressed on tumors. Molecular imaging has emerged as a novel multidisciplinary field that provides potential for earlier detection and characterization of disease, elucidation of mechanisms at the molecular level, and evaluation of therapy by use of specific molecular probes. Advantages of such molecular imaging approaches include noninvasiveness and the ability to measure both spatial and temporal biodistribution of a molecular probe in intact living subjects for real time and serial studies.

Correspondence to: Mathew L. Thakur.

Publisher's Disclaimer: This is a PDF file of an unedited manuscript that has been accepted for publication. As a service to our customers we are providing this early version of the manuscript. The manuscript will undergo copyediting, typesetting, and review of the resulting proof before it is published in its final citable form. Please note that during the production process errors may be discovered which could affect the content, and all legal disclaimers that apply to the journal pertain.

Analysis of genomic sequence data generated by the human genome project is expected to give a better understanding of the genes involved in cancer development and chronic diseases [1]. Recent research reveals cancer to be a disease involving dynamic changes in the genome. Mutations that produce oncogenes with dominant gain of function and tumor suppressor genes with recessive loss of function have been identified for elicitation of cancer phenotypes in several cancers [2]. Modulations in the expression of key proteins of the cellular signaling pathways are at the forefront of molecular abnormalities found in cancer. Protein products of proto-oncogenes and tumor suppressor genes are involved in cell growth as growth factors, receptors, intracellular mediators or transcription factors and have been found to be altered through multiple mechanisms of oncogene activation. These include enhanced or ectopic expression, deletions, single point mutations and generation of chimeric proteins [3]. Considerable success has been achieved in the development of molecular imaging agents based on peptide–receptor, antibody–antigen, and substrate–enzyme interactions targeting such overexpressed or mutated proteins in cancers [4,5,6]. However, due to tertiary folding and complex structures in each individual protein, it is not feasible to design ligands for any protein based on peptide sequences alone.

Antisense chemotherapy based on the complementary hybridization of an antisense with a target oncogene mRNA sequence is being exploited for treatment of various types of cancers [7]. Based on the same targeting principle, radiolabeled antisense sequences have been explored for imaging applications. Design of antisense sequences for mRNA is theoretically straightforward, based on complementary base pairing rules. Noninvasive, real time imaging of oncogene expression in vivo would provide information on cellular gene expression patterns and might reveal molecular changes in diseased tissues at relatively early stages providing opportunities for gene therapy, especially against overexpressed oncogene mRNAs [8]. In this approach of mRNA targeting, high specificity may be achieved upon binding of radiolabeled oligonucleotides to the target due to sequence complementarity [9]. This approach is not only specific but also sensitive as it has been proposed that mRNA concentrations as low as 1pmol/L in the tissues can probably be imaged with positron emission tomography (PET) using radiolabeled probes of specific activity 1000 to 10000 Ci/mmol [10]. However, there are challenges in imaging endogenous gene expression with radiolabeled oligonucleotides such as in vivo stability, transport to the target, entry into the cell and hybridization with target specific sequences [11]. Development of antisense imaging agents is in its infancy, compared to other approaches of molecular imaging. However, imaging with antisense technology for early, specific and noninvasive detection of oncogene expression is unique and warrants greater attention.

2. Cancer diagnosis via endogenous gene expression

Out of the 20,000 to 25,000 genes in human genome, about 100 have been identified as protooncogenes and tumor suppressor genes [12] *CCND1*, *HER2*, *MYCC*, *KRAS* and *BCL2* oncogenes, as well as the tumor suppressor *TP53*, are reported to be frequently mutated or overexpressed in cancer cells.

HER2 oncogene, also known as *ERBB2/neu*, encodes a transmembrane glycoprotein, Her2 (185kDa) with tyrosine kinase activity. Amplification of Her2 expression, consequent to gene amplification, has been demonstrated in a subset of breast cancers corresponding to approximately one third of the patients affected by the disease [13]. Overexpression of Her2 is also reported in other human tumors including ovarian carcinomas, head and neck cancer, lung and gastro-intestinal tumors [14]. Specific down regulation of *HER2* mRNA and protein by antisense phosphorothioate oligonucleotide is reported indicating possibility of *HER2* mRNA as a specific target for tumor imaging [15].

Activated *RAS* oncogenes have been identified in precancerous lesions of some common forms of human cancers indicating their role in early stages of carcinogenesis. *HRAS* mutation is most often associated with bladder and kidney cancers, *NRAS* mutations with melanoma and hematological malignancies, and *KRAS* mutations with lung, colorectal, ovarian and pancreatic cancers [16]. The human *KRAS* proto-oncogene codes for an evolutionary conserved G protein, K-Ras p21, which binds guanine nucleotides with high affinity and is associated with the inner surface of the plasma membrane. K-Ras p21 is involved in transducing signals from growth factors binding to the cell surface receptors [17]. Point mutations in *KRAS* proto oncogene, mostly confined to codon 12 or 13, are reported to be an early event in pancreatic tumorigenesis indicated both by high gene mutation frequency and by the presence of mutation in low grade tumors [18]. Approximately 95% of ductal pancreatic cancers exhibit activation of *KRAS* oncogene at the early pancreatic intraepithelial neoplasia (PanIN-1) stage [19].

MYCC oncogene encodes a nuclear DNA binding protein c-Myc (65 kDa) that binds with a small partner protein, Max. The resulting heterodimer binds specifically to the promoter element in the regulatory regions of genes involved in proliferation. *MYCC* oncogene expression is stimulated by estrogen in hormone responsive breast cancer cells in vitro. Amplification of *MYCC* is considered to be a powerful prognostic indicator, particularly in node negative and estrogen receptor positive breast cancer [20]. *MYCC* was the first oncogene targeted by antisense, specifically by MYC6 sequence to treat HL-60 promyelocytic leukemia cells. Gene inhibition and antiproliferative activity were displayed by MYC6 sequence in breast cancer cells [21].

Cyclin D1 protein, encoded by *CCND1* (*BCL1*, *PRAD1*), is a proto-oncogenic regulator of the G1/S checkpoint in the cell cycle that has been implicated in the pathogenesis of several types of cancers, including breast, prostate, and pancreatic cancer [22]. Cyclin D1 appears to function by binding to cyclin dependent kinases. Overexpression of cyclin D1 in cultured cells leads to a more rapid transition through the G1 phase of the cell cycle and entry into the S phase.

Another oncogene involved in initiation of almost all follicular lymphomas and some diffuse large B-cell lymphomas is *BCL2*. This gene encodes a cytoplasmic protein that localizes to mitochondria and increases cell survival by inhibiting apoptosis. *BCL2* is also important in chronic lymphocytic leukemia and lung cancer. The *BCL2* family members *BCL-XL* and *BCL2* inhibit apoptosis and are upregulated in many cancers [23,24,25]. Mutations in p53, a tumor suppressor gene has been found to be the most frequent genetic alteration in diverse types of human cancers [26].

Oligonucleotide antisense sequences specific for *CCND1* [27], *HER2* [15], *MYCC* [28], *KRAS* [29], *BCL2* [30] and *TP53* [31] are reported to downregulate respective gene expression in cancers. Hence, mutated or overexpressed *CCND1*, *HER2*, *MYCC*, *KRAS*, *BCL2*, and *TP53* mRNAs are expected to serve as potential markers when linked with suitable radionuclides, fluorophores, or contrast agents for nuclear, optical, or magnetic resonance imaging, respectively.

3. In vivo gene imaging agents

Many challenges must be overcome for successful development of imaging agents for gene expression, such as improvement in chemistry to achieve stable oligonucleotides, and conjugation of oligonucleotides to the signaling moieties. Cell specific targeting of antisense sequences and development of biologically compatible probes to facilitate translation of in vitro results to in vivo applications is desired. There is also a need to address mechanisms of cellular uptake of oligonucleotides and estimate hybridization specificity of radiolabeled antisense agents [32].

3.1 Stability

Success has been achieved in design and synthesis of stable oligonucleotides based on modifications in the phosphate backbone, sugar, and heterocyclic base of nucleic acid monomers [33]. Novel oligonucleotide analogs have been synthesized with improved biological stability, solubility, cellular uptake and ease of synthesis. The simplest oligodeoxynucleotide modification involved blocking the 3' terminus to prevent attack by 3' exonucleases, the predominant extracellular degradative mechanism for oligodeoxynucleotides [34]. Other modifications focused on protecting the internucleoside linkage by changing the phosphodiester linkages to phosphorothioates, methylphosphonates, or boranophosphates [35]. Although these modifications have led to increased in vivo stability of oligonucleotides, they also have weakened hybridization to the RNA target sites due to the creation of chiral phosphorus diastereomers [36]. The deoxyribose may be modified to 2'-O-alkyl RNAs, such as 2'-O-methyl, strengthening hybridization and resisting nuclease attack [37]. Similar improvements result from preparing 3'-amino phosphoramidates or morpholino phosphorodiamidates [35].

Furthermore, attachment of a base to deoxyribose may be reversed, changing the natural β -anomer to the α -anomer. The α -anomer achieves nuclease resistance without loss of base pairing [38]. Each of these structural changes affect not only the nuclease susceptibility, but also the cellular uptake, the cellular trafficking and recognition as substrate for RNase H [39]. Among the derivatives described, only phosphodiester, phosphorothioates, and boranophosphates DNAs direct RNase H mediated degradation of hybridized RNA. Encouraging results have been obtained suggesting that greater potency and a better specificity might be possible with 2'-O-alkyl RNA, phosphorothioate chimeras, anomeric DNA chimeras, or DNA boranophosphates [35,40].

The most radical modifications to oligonucleotides are found in peptide nucleic acids (PNA), where both the phosphodiester linkages and sugars are replaced with a peptide-like backbone of (N-2-aminoethyl) glycine units, with the bases directly attached by methylene-carbonyl linkers. Due to their achiral, uncharged and rather flexible peptide backbone, PNAs hybridize more strongly and specifically to RNA [41]. Twelve PNA bases are reported to be sufficient for statistical uniqueness among transcribed mRNAs [42]. Compared with other oligonucleotide derivatives, PNAs display the highest melting temperature (T_m) for duplexes formed with single-stranded DNA or RNA [42]. PNAs are not easily recognized by either nucleases or proteases and are thus resistant to enzymatic degradation and also show stability over a wide range of pH [43]. Hence, PNAs show desired properties for development of antisense imaging agents.

3.2 Antisense mechanism

Antisense oligonucleotides have shown promising results as chemotherapeutic agents. However, phosphorothioate DNAs are the only derivatives that have thus far been administered to humans. Despite their efficacy, phosphorothioate (PS) DNAs exhibit less sequence specificity than phosphodiester or methylphosphonates due to significant binding to a wide spectrum of plasma and cellular proteins [44]. Requirements for antisense chemotherapy are different than those for antisense imaging. Pharmacokinetic requirements differ sharply as the antisense cellular transport is limited and mRNAs are produced continuously. For chemotherapy, prolonged blood circulation of antisense is desired to eliminate need for multiple administrations while for antisense imaging, rapid plasma clearance for achieving high target to background ratio is required. Among the chemically modified oligonucleotides such as phosphorothioates, a positive correlation exists between their ability to act as substrates for RNaseH due to formation of a suitable RNA: DNA hybrid and their potency for antisense inhibition. This indicates RNaseH-mediated translational arrest as a major mechanism of

antisense chemotherapy [11]. However, for antisense imaging, hybridization of probe to the target sequence is the principal requirement. RNA hybridized to uncharged oligonucleotide derivatives, such as PNA, is not recognized and cleaved by RNase H. Hence, PNAs are more promising for diagnostic applications than the charged derivatives because the PNAs, the analytical reagents, do not destroy the target mRNA, the analyte.

3.3 Cell specific targeting of antisense sequences

A number of delivery systems for oligonucleotide transport have been reported. These are lipid-based agents, polypeptides, polylysines, recombinant histones and biotinylated polyamidoamine dendrimers. Among them biotinylated polyamidoamine dendrimers have emerged as novel cationic gene carriers [45,46]. However, these agents are not specific for tumor cells.

Cellular uptake and nuclear localization are also reported to be dependent on the type of modification in the oligonucleotide sequence. Cellular accumulation of phosphorothioates is reported to be 3–5 fold more than 3'-alkylamino oligodeoxynucleoside phosphodiester (PONH₂) and 2'-O-methyl oligoribonucleotide phosphodiester (2 OM), 6–7 fold greater than PNAs and 8–10 fold more than oligodeoxynucleoside methylphosphonates [47]. The relative hybridization efficiency to the target sequence ranged in the order 2'-O-methyl phosphodiester (OMe) > phosphodiester (PO) and phosphorothioate (PS) [48].

To improve the uptake of PNAs specifically in tumor cells, PNAs linked to peptide ligands of receptors overexpressed on tumor cells were explored. Peptides such as IGF-1 analogues and Tyr³-ocreotate have been coupled to antisense sequences to improve cell delivery [49,50]. Dihydrotestosterone attached to anti-gene PNA (Anti-DNA PNA) was reported to be a selective cellular/nuclear localization vector in prostate cancer cells, correlating with recent suggestions of membrane presentation of androgen receptors [51]. General, nonspecific cell penetrating peptides such as polylysine, oligolysine, and membrane permeating transducing peptide PTD-4 have also been coupled to antisense sequences to improve cell delivery [52,53].

3.4 Radiolabeling

Methods for radiolabeling antisense agents with beta emitters such as ³H, ³⁵S and ³²P are well established. Methods for synthesis of oligonucleotides ready to be labeled with radionuclides for imaging applications are also very well reported.

Because of favorable decay properties and availability, ^{99m}Tc remains a radionuclide of choice for SPECT imaging. Radiolabeling with ^{99m}Tc has been reported using various chelating groups attached to oligonucleotide sequences. Diethylene triamine pentaacetic acid (DTPA), 6-hydrazinonicotinamide (HNH), and mercaptoacetyl-triglycine (MAG₃) conjugated to oligonucleotides have been reported for chelation of ^{99m}Tc as well as for ¹¹¹In labeling [9, 54,55]. A facile method for labeling PNA ligands with ^{99m}Tc was reported using a tetrapeptide, Gly-D-Ala-Gly-Gly, providing an N₄ conformation for strong and efficient chelation of ^{99m}Tc [56]. Radioiodination of oligonucleotides has been reported using tributylstannyl benzamide and p-methoxyphenyl isothiocyanate (PMPITC) conjugates [57].

With the success achieved in PET imaging due to high resolution and sensitivity, a number of positron emitting radionuclides are being employed as tracers. The macrocyclic chelator, 1, 4,7,10 tetraaza cyclododecane tetraacetic acid (DOTA) conjugated to antisense sequences has been utilized for complexation with positron emitters such as ⁶⁴Cu and ⁶⁸Ga [58,59,60]. DOTA was also reported for radiolabeling of gamma and beta emitting radionuclides such as ¹¹¹In and ⁹⁰Y [53]. Probes with an N₂S₂ chelator were also reported for ⁶⁴Cu labeling. Diaminopropionic acid was incorporated at the N terminus of the PNA with an

aminoethoxyethoxyacetic acid linker (AEEA) coupled to two S-benzoyl thioglycolic acid residues (SBTG₂) to generate an N₂S₂ chelator [61]. Dendrimeric chelator-PNA-peptide probes have been utilized for MRI using Gd (III) as a contrast agent [62].

Synthons are structural units that can be incorporated as part of the synthesis of a larger molecule. Synthons can be radiolabeled prior to synthesizing a molecular probe. Methods for labeling with radiohalogens, mostly positron and gamma emitters like ¹⁸F, ¹³¹I, and ⁷⁶Br, typically involve prelabeling of synthons for high yield and stable incorporation of halogens [63]. Purification of the synthon from other radioactive byproducts is done by HPLC followed by regioselective conjugation of the radiolabeled synthon to an oligonucleotide. Prelabeling provides the possibility to work with any oligonucleotide synthesized in house or commercially without tedious unblocking steps [48]. It was reported that the hybridization efficiency of radiolabeled antisense oligonucleotides was not compromised due to the method of radiolabeling [63].

3.5 Pharmacokinetics of antisense agents

Pharmacokinetics of various antisense agents labeled with ¹⁸F and ⁶⁸Ga using different backbones such as phosphodiester (PO), phosphorothioate (PS) and 2'-O-methyl phosphodiester (OMe) were studied and observed to be dependent on oligonucleotide backbone [63,64,65]. Tissue distribution of the radioactivity showed that the phosphodiester was eliminated both through renal and digestive system while phosphorothioates and 2'-O-methyl RNAs showed only renal excretion [63]. Pharmacokinetics of uncharged PNAs linked to tumor targeting peptides is expected to be governed by the specificity of the peptide for the receptors expressed on tumor cells.

Like development of any new radiopharmaceutical, antisense imaging agents need to undergo intense, systemic and thorough evaluation before they can be used in clinics. Table 1 summarizes the major steps in the research and development of antisense imaging agents. Perhaps the most important aspect is preferential uptake by the target tissue and ability of the probes to hybridize specifically to the target mRNA sequences.

4. Pioneer oncogene expression imaging investigations

A number of oncogenes like *KRAS*, *HER2* (*ERB-B2*, *neu*), *MYCC*, *BCL2* and *CCND1* are overexpressed in various types of cancers. Among them, breast and pancreatic cancers have been targeted using radiolabeled antisense probes [8]. Apart from detection of cancers based on overexpression of genes, this technology was also explored for determination of response to anticancer therapy. This was accomplished by studying the expression of an early response gene for DNA damage, p21^{WAF-1/CIP-1} [66].

One investigation demonstrated preferential in vitro uptake and retention of radiolabeled antisense in tumor cells. A 18mer phosphorothioate antisense to the initiation codon of the *HER2* oncogene mRNA was synthesized. The sense strand was also synthesized and both were labeled with ³²P. The uptake and retention of radiolabeled antisense *HER2* was observed in MCF-7 cells known to express *HER2* mRNA. However, studies to show target-specific uptake and in vivo distribution of the agent were not performed [67]. A similar in vitro study reported hybridization of ^{99m}Tc and ³²P labeled 15mer phosphodiester oligodeoxynucleotide antisense to the complementary *MYCC* sequence. Efficient binding to the complementary sequence was achieved in cell-free systems. However, uptake in a cell line expressing *MYCC* and in a *MYCC* knockout cell line was not statistically different [68]. A 23mer oligonucleotide phosphodiester sequence, complementary to the translation initiation site of TGF- α mRNA, was radiolabeled with ¹²⁵I [69]. Radioiodination was achieved via a tyramine group conjugated to the 5' end. In this study, a FITC labeled 23mer TGF- α antisense was used to demonstrate in

vitro stability, intracellular and nuclear localization in NS2T2A1 cells, expressing high levels of TGF- α . In in vivo studies, uptake was followed after intratumoral injection. Tumor uptake ranged from 14% at 1 h to 1.2% at 24 h p.i. No study to indicate uptake and retention via antisense mechanism was performed [69].

Synthesis and bioevaluation of a 15mer phosphodiester and a 15mer phosphothioate DNA complementary to a sequence within the initiation codon site of *MYCC* oncogene mRNA was reported [10,55]. Sequences were conjugated to a DTPA analogue and were labeled with ^{111}In . Uptake of the radiolabel in murine monocyte leukemia tumor cells appeared to be significantly higher for antisense DNAs compared to sense DNAs. In nude mice bearing mammary adenocarcinoma xenografts, 10 to 12% uptake of radiolabeled antisense DNAs was observed in the tumors as compared to 1% uptake of the sense sequence at 1 h p.i. However, uptake in blood and muscles were 18–20% and 15–17% respectively. Such high uptake might lead to high background and hinder in achieving good scintigraphic images for tumor detection [55]. However, no subsequent investigations verifying the above results have been reported.

Another study reported ^{68}Ga -labeled 17mer oligonucleotide sequences for targeting mutated *KRAS* oncogene mRNA in human A549 lung cancer xenografts. The intravenously injected tracer revealed high quality PET images that allowed quantification of biokinetics in major organs and in tumors containing *KRAS* point mutations versus tumors with wild type *KRAS* oncogene [65].

In the recent past, peptide nucleic acid based antisense sequences labeled with $^{99\text{m}}\text{Tc}$, ^{111}In , ^{64}Cu and ^{90}Y showed promising results for targeting oncogene mRNA. In one study, beads conjugated with a complementary DNA sequence were first injected in the thigh region of the mice. A $^{99\text{m}}\text{Tc}$ labeled PNA sequence was then administered i.v. The PNA probe showed stability and superior pharmacokinetics along with high uptake in the left thigh where the complementary DNA beads were located [9].

Synthesis and characterization of PNA probes with a peptide analog of insulin-like growth factor 1 (IGF1) for increased tumor cell uptake and chelating groups for $^{99\text{m}}\text{Tc}$ and ^{64}Cu labeling have been studied extensively [70]. A construct of chelator-PNA-peptide is depicted in Figure 1. Antisense sequences specific for *CCND1* [71] and *MYCC* [72] mRNAs were explored for genetic characterization of breast cancer xenografts. Unique PNA sequences targeting the initiation codon regions were selected because the start codon domain has been reported to be available for PNA hybridization.

An antisense sequence for the *KRAS* D12 mutant was selected for targeting *KRAS* oncogene expression in pancreatic cancer xenografts. In this study, PNA sequences targeting the mutated 12th codon region of *KRAS* oncogene mRNAs were selected [73]. Probes with 12mer antisense sequence and 12mer mismatch controls for *CCND1*, *KRAS* and *MYCC* were synthesized because PNA oligomers as short as 12 residues are reported to be sufficient for statistical uniqueness [8]. Sequences with one, two, three mismatch served as controls. Hydrophilic aminoethoxyethoxyacetyl (AEEA) and 4-aminobutanoyl (Aba) spacers were introduced at the N terminus and C terminus of PNA hybridization sequences to minimize the steric hindrance of bulky chelator-metal ion complex and the cyclic peptide moieties. Without the spacers, these bulky groups might affect the hybridization efficiency of the PNAs. To achieve tumor cell specificity and improved cellular delivery of PNAs, the IGF1 analog JB9, cyclic D- (Cys-Ser-Lys-Cys), was extended from the solid phase support before coupling of the hydrophilic spacer and the PNA monomers. N_4 chelation of $^{99\text{m}}\text{Tc}$ was achieved by extending a tetrapeptide, Gly-D-Ala-Gly-Gly, from the N terminus of the spacer-PNA-spacer-peptide. Probes with either DO3A or an N_2S_2 chelator coupled to the N-termini of spacer-PNA-spacer-peptides were

synthesized for ^{64}Cu labeling. Their sequences are shown in Table 2. Schematics of chelator-PNA-peptides labeled with $^{99\text{m}}\text{Tc}$, ^{64}Cu and Gd are displayed in Figure 2.

Although PNAs are internalized poorly into mammalian cells, *CCND1* fluoresceinyl-PNA-IGF1 peptide probe was internalized efficiently by cells overexpressing IGF1 receptors, compared to a peptide mismatch probe [8,49]. Scintigraphic imaging of MCF-7 xenografts in immunocompromised mice revealed 7-fold higher intensity of *CCND1* and *MYCC* $^{99\text{m}}\text{Tc}$ -chelator-PNA-D(Cys-Ser-Lys-Cys) probes compared to mismatch or contralateral controls [71,72]. Figure 3 depicts uptake of $^{99\text{m}}\text{Tc}$ -*CCND1* PNA-peptide probe in MCF-7 xenografts in nude mice at 4, 12, 24 h p.i. [71]. A specific ^{64}Cu -DO3A-*CCND1* PNA-IGF1 analog radiohybridization probe was injected intravenously into immunocompromised mice bearing breast cancer xenografts. Eight-fold higher PET intensity at the center of breast cancer xenograft was observed compared to intensity in the contralateral tissues at 24 h p.i. PNA mismatch, peptide mismatch probe and IGF1 blocking yielded significantly weaker images [60].

An SBTG₂-DAP-PNA-IGF1 analog antisense probe for mutant *KRAS* mRNA was labeled with $^{99\text{m}}\text{Tc}$ and also with ^{64}Cu . The radiometal-chelator-PNA-peptide hybridization probes were injected intravenously into immunocompromised mice bearing pancreatic cancer xenografts, followed by scintigraphic and PET imaging [8]. ^{64}Cu -DO3A-*KRAS* PNA-IGF1 analog (WT4286) radiohybridization probe that was specific for the D12 *KRAS* mutation in human ASPC1 pancreatic cancer cells gave strong tumor contrast. Eight-fold increase in intensity at the centre of human pancreatic cancer xenografts in PET images was observed compared to the intensity in the contralateral muscle at 4 h p.i as shown in Figure 4 [73]. These results are encouraging and suggest a promising future for early and specific imaging of malignant lesions.

^{111}In and ^{90}Y labeled PNA complementary to the first six codons of *BCL2* mRNA were reported. Membrane permeating transducing peptide PTD-4 was coupled to PNA for intracellular delivery. DOTA served as chelating moiety in the probe. ^{90}Y -PTD-4-K (DOTA) – anti *BCL2* PNA showed binding similar to ^{32}P labeled analogues when northern analysis was performed using *BCL2* mRNA from a cell free system [53]. The same group recently reported an ^{111}In labeled anti *BCL2* sequence coupled to Tyr³-octreotate for somatostatin receptor mediated intracellular delivery. Tumors could be imaged by ^{111}In -DOTA-anti *BCL2*-PNA-Tyr³-octreotate at 48h p.i. [50].

MicroPET imaging of MCF-7 tumors in mice was reported using PNA targeting murine unr mRNA (upstream of *NRAS*) sequence. Tetralysines were incorporated at the carboxy termini for cell permeation and PNA was coupled to DOTA for ^{64}Cu labeling. ^{64}Cu -DOTA-Y-PNA50-K4 showed good uptake in tumors with tumor/muscle ratio of 6.6 ± 1.1 at 24 h p.i [52]. Nevertheless, sequence-specific tumor images were not observed. The negative results were ascribed to mouse tissue expression of murine unr mRNA with the same target sequence as human *UNR* mRNA, and uptake of the PNA universally in all cells due to the nonspecific Lys₄ tail.

These studies strengthen the potential of radiolabeled antisense PNAs for utilization as specific molecular probes for early detection of cancer and ultimately for disease specific radiotherapy.

5. Perspectives

Cancer remains the most formidable disease of mankind. Early detection of cancer following effective therapeutic intervention can save lives. Advances in genomics and proteomics are being reported almost every day, shedding new light on the genesis of cancer. Targeting specific

biomarkers with radiohybridization probes may play a significant role in early detection of cancer.

Success has been achieved in design and synthesis of novel antisense agents with improved stability and binding affinity. Availability of automated technology for synthesis of antisense agents and recent reports on possibility of single, continuous, solid phase synthesis of various peptide-PNA conjugates indicates the possibility of large scale synthesis of conjugates for commercial applications.

Promising results have been achieved in cell free systems and to some extent in *in vitro* systems. For *in vivo* applications, limited success has been achieved. Furthermore, many issues such as *in vivo* stability, target cell specificity, uptake and retention in the cell and interaction with the target sequences need to be established. Future studies are needed to validate the hypothesis of specificity of the radio hybridization probes to the target sequences in *in vitro* and *in vivo* systems. Whether the uptake and retention of antisense agents is proportional to the expression of intracellular message needs to be addressed. Apart from the use of radionuclides for labeling oligonucleotides and PNAs, newer signaling moieties like near infrared (NIR) dyes for optical imaging and supermagnetic iron oxide for magnetic resonance imaging may be useful for *in vivo* imaging. However, in such approaches, depth and sensitivity are major concerns. Use of dendrimers, conjugated to antisense sequence for incorporation of multiple labels may be helpful in improving the signal for diagnostic applications. These may also be useful for therapeutic applications when labeled with radionuclides of therapeutic importance.

Molecular imaging of oncogene mRNAs with novel and improved hybridization probes for early, specific and noninvasive detection of cancers warrants greater attention.

Acknowledgements

This research was supported by NIH CA109231, EB001809, 1S10RR23709 and PA ME-03-184 grants to M.L.T., and DOE ER63055 and NIH C027175 to E.W.

References

1. Weissleder R, Mahmood U. Molecular Imaging. *Radiology* 2001;219:316–33. [PubMed: 11323453]
2. Hanahan D, Weinberg RA. The Hallmarks of Cancer. *Cell* 2000;100:57–70. [PubMed: 10647931]
3. Weinberg RA. How cancer arises. *Sci Am* 1996 sept;:62–70. [PubMed: 8701295]
4. Mankoff DA, Link JM, Linden HM, Sundararajan L, Krohn KA. Tumor receptor imaging. *J Nucl Med* 2008;49:149S–63S. [PubMed: 18523071]
5. Plathow C, Weber WA. Tumor cell metabolism imaging. *J Nucl Med* 2008;49:43S–63S. [PubMed: 18523065]
6. Krohn KA, Link JM, Mason RP. Molecular imaging of hypoxia. *J Nucl Med* 2008;49:129S–48S. [PubMed: 18523070]
7. Gleave ME, Monia BP. Antisense therapy for cancer. *Nature Reviews Cancer* 2005;5:468–79.
8. Tian, X.; Chakrabarti, A.; Amirkhanov, N., et al. External imaging of *CCND1*, *MYC* and *KRAS* oncogene mRNAs with tumor-targeted radionuclide-PNA-peptide chimeras. In: El-Deiry, W., editor. *Ann N Y Acad Sci*. Vol. 1059. 2005. p. 106–44.
9. Mardirossian G, Lei K, Rusckowski M, Chang F, Qu T, Egholm M, Hnatowich DJ. *In vivo* hybridization of technetium-99m-labeled peptide nucleic acid (PNA). *J Nucl Med* 1997;38:907–13. [PubMed: 9189140]
10. Dewanjee MK, Haider N, Narula J. Imaging with antisense oligonucleotides for the detection of intracellular messenger RNA and cardiovascular disease. *J Nucl Cardiol* 1999;6:345–56. [PubMed: 10385190]
11. Hnatowich DJ. Antisense and nuclear medicine. *J Nucl Med* 1999;40:693–703. [PubMed: 10210231]

12. Pickeral OK, Li JZ, Barrow I, Boguski MS, Makalowski W, Zhang J. Classical oncogenes and tumor suppressor genes: A Comparative genomics perspective. *Neoplasia* 2000;2(3):280–86. [PubMed: 10935514]
13. Revillion F, Bonnetterre J, Peyrat JP. ERBB2 oncogene in human breast cancer and its clinical significance. *Eur J Cancer* 1998;34(6):791–808. [PubMed: 9797688]
14. D'Incalci M. Correlation of ErbB2 gene status, mRNA and protein expression. *Onkologie* 2006;29:246–7. [PubMed: 16770085]
15. Vaughn JP, Iglehart JD, Demirdji S, et al. Antisense DNA down regulation of the ERBB2 oncogene measured by a flow cytometric assay. *Proc Natl Acad Sci USA* 1995;92:8338–42. [PubMed: 7667291]
16. Bos JL. Ras oncogenes in human cancer: A review [published erratum appears in *Cancer Res* 1990 Feb 15; 50(4): 1352]. *Cancer Res* 1989;49:4682–9. [PubMed: 2547513]
17. Lowy DR, Willumsen BM. Function and regulation of ras. *Annu Rev Biochem* 1993;62:851–91. [PubMed: 8352603]
18. Pellagata NS, Sessa F, Renault B, et al. K-ras and p53 gene mutations in pancreatic cancer: Ductal and Nonductal tumors progress through different genetic lesions. *Cancer Res* 1994;54:1556–60. [PubMed: 8137263]
19. Evans, DB.; Abbruzzese, JL.; Willett, CG. Cancer of pancreas. In: Devita, VT.; Hellman, S.; Rosenberg, SA., editors. *Cancer: Principles and practice of Oncology*. Philadelphia: Lippincott, Williams and Wilkins; 2001. p. 1126-61.
20. Berns Els MJJ, Klijn JGM, van Staveren IL, Portengen H, Foekens JA. *c-myc* amplification is a better prognostic factor than *Her2/neu* amplification in primary breast cancer. *Cancer Res* 1992;52:1107–13. [PubMed: 1737370]
21. Wickstrom EL, Bacon TA, Gonzalez A, Freeman DL, Lyman GH, Wickstrom E. Human promyelocytic leukemia HL-60 cell proliferation and c-Myc protein expression are inhibited by an antisense pentadecadeoxynucleotide targeted against c-MYC mRNA. *Proc Natl Acad Sci USA* 1988;85(4):1028–32. [PubMed: 3277186]
22. Weinstat-Saslow D, Merino MJ, Manrow RE, et al. Overexpression of cyclin D mRNA distinguishes invasive and in situ breast carcinomas from non-malignant lesions. *Nat Med* 1995;1:1257–60. [PubMed: 7489405]
23. Hermine O, Haioun C, Lepage E, et al. Prognostic significance of bcl-2 protein expression in aggressive Non-Hodkins lymphoma. *Blood* 1996;87:265–72. [PubMed: 8547651]
24. Pepper C, Bentley P, Hoy T. Regulation of clinical chemo resistance by bcl-2 and bax oncoproteins in B-cell chronic lymphocytic leukemia. *Br J Haematol* 1996;95:513–17. [PubMed: 8943893]
25. Croce CM. Oncogenes and cancer. *N Engl J Med* 2008;358:502–11. [PubMed: 18234754]
26. Hollstein M, Sidransky D, Vogelstein B, Harris CC. p53 mutations in human cancers. *Science* 1991;253:49–53. [PubMed: 1905840]
27. Sauter ER, Herlyn M, Liu SC, Litwin S, Ridge JA. Prolonged response to antisense cyclin D1 in a human squamous cancer xenograft model. *Clin Cancer Res* 2000;6:654–60. [PubMed: 10690551]
28. Wickstrom E, Bacon TA, Wickstrom EL. Down regulation of c-MYC antigen expression in lymphocytes of Eμ-c-myc transgenic mice treated with anti-c-myc DNA methylphosphonates. *Cancer Res* 1992;52:6741–45. [PubMed: 1458461]
29. Wickstrom, E. *Clinical trials of genetic therapy with antisense DNA and DNA vectors*. New York: Marcel Dekker; 1998.
30. Webb A, Cunningham D, Cotter F, et al. BCL-2 antisense therapy in patients with non-Hodgkin lymphoma. *Lancet* 1997;349:1137–41. [PubMed: 9113013]
31. Bayever E, Haines KM, Iversen PL, et al. Selective cytotoxicity to human leukemic myoblasts produced by oligodeoxyribonucleotide phosphorothioates complementary to p53 nucleotide sequences. *Leuk Lymphoma* 1994;12:223–26. [PubMed: 8167553]
32. Paroo Z, Corey DR. Imaging gene expression using oligonucleotides and peptide nucleic acids. *J Cell Biochem* 2003;90:437–42. [PubMed: 14523977]
33. Swayze, EE.; Balkrishen, B. The medicinal chemistry of oligonucleotides. In: Croke, ST., editor. *Antisense drug technology: Principles, strategies and applications*. CRC press; USA: 2008. p. 144-72.

34. Zendejui JG, Vazquez KM, Tindley JH, et al. In vivo stability and kinetics of absorption and disposition of 3' phosphopropyl amine oligonucleotides. *Nucleic acids Res* 1992;20(2):307–14. [PubMed: 1741256]
35. Thakur ML, Tian X, Amirkhanov N, et al. The role of radiolabeled peptide nucleic acid chimeras and peptides in imaging oncogene expression. *Indian J Nucl Med* 2004;19(3):98–114.
36. Lebedev, AV.; Wickstrom, E. The chirality problem in P-substituted oligonucleotides. In: trainor, G., editor. *Perspectives in Drug Discovery and Design*. Leiden: ESCOM science publishers; 1996. p. 17-40.
37. Monia BP, Lesnik EA, Gonzalez C, et al. Evaluation of 2' modified oligonucleotides containing 2'-deoxy gaps as antisense inhibitors of gene expression. *J Biol Chem* 1993;268:14514–22. [PubMed: 8390996]
38. Bacon TA, Morvan F, Rayner B, et al. Alpha-oligodeoxynucleotide stability in serum, subcellular extracts and culture media. *J Biochem Biophys Methods* 1988;16(4):311–8. [PubMed: 3221039]
39. Ho PT, Ishiguro K, Wickstrom E, et al. Non-sequence-specific inhibition of transferrin receptor expression in HL-60 leukemia cells by phosphorothioate oligodeoxynucleotides. *Antisense Research & Development* 1991;1(4):329–42. [PubMed: 1821654]
40. Cook, D. Antisense medicinal chemistry. In: Crooke, ST., editor. *Antisense research and applications*. Berlin-Heidelberg: Springer-Verlag; 1998. p. 51-92.
41. Good L, Nielsen PE. Progress in developing PNA as a gene targeted drug. *Antisense Nucleic Acid Drug Dev* 1997;7(4):431–37. [PubMed: 9303195]
42. Tian X, Wickstrom E. Continuous solid phase synthesis and disulfide cyclization of peptide-PNA-peptide chimeras. *Org Lett* 2002;4:4013–16. [PubMed: 12423074]
43. Nielsen, PE. Antisense properties of peptide nucleic acids. In: Crooke, ST., editor. *Antisense research and applications*. Berlin-Heidelberg: Springer-Verlag; 1998. p. 545-57.
44. Agrawal S. Antisense oligonucleotides: towards clinical trials. *Trends in Biotechnology* 1996;14(10):376–87. [PubMed: 8987636]
45. Olivier, S.; Bolard, J. Delivery agents for oligonucleotides. In: Sioud, M., editor. *Methods in Molecular Biology*. Vol. 252. Totowa, New Jersey: Humana Press; 2004. p. 545-68. Ribozymes and siRNA protocols
46. Sato N, Kobayashi H, Saga T, et al. Tumor targeting and imaging of intraperitoneal tumors by use of antisense oligo-DNA complexed with dendrimers and/or avidin in mice. *Clin Can Research* 2001;7:3606–12.
47. Gray GD, Basu S, Wickstrom E. Transformed and immortalized cellular uptake of oligodeoxynucleoside phosphorothioates, 3' Alkylamino oligodeoxynucleosides, 2'-O-methyl oligoribonucleotides, Oligodeoxynucleosides methyl phosphonates, and peptide nucleic acids. *Biochem Pharmacol* 1997;53:1465–76. [PubMed: 9260874]
48. Tavittian B, Terrazzino S, Kuhnast B, et al. In vivo imaging of oligonucleotides with positron emission tomography. *Nat Med* 1998;4(4):467–71. [PubMed: 9546795]
49. Basu S, Wickstrom E. Synthesis and characterization of a peptide nucleic acid conjugated to a D-peptide analog of insulin like growth factor1 for increased cellular uptake. *Bioconj Chem* 1997;8:481–88.
50. Jia F, Figueroa SD, Gallazzi F, et al. Molecular imaging of bcl-2 expression in small lymphocytic lymphoma using ¹¹¹In-labeled PNA-peptide conjugates. *J Nucl Med* 2008;49:430–38. [PubMed: 18287262]
51. Boffa LC, Scarfi S, Mariani MR, et al. Dihydrotestosterone as a selective cellular/nuclear localization vector for anti-Gene peptide nucleic acid in prostatic carcinoma cells. *Cancer Res* 2000;60:2258–62. [PubMed: 10786693]
52. Sun X, Fang H, Li X, et al. MicroPET imaging of MCF-7 tumors in mice via unr mRNA targeted peptide nucleic acids. *Bioconj Chem* 2005;16:294–305.
53. Lewis MR, Jia F, Gallazzi F, et al. Radiometal-labeled peptide-PNA conjugates for targeting bcl-2 expression: Preparation, characterization and in vitro mRNA binding. *Bioconj Chem* 2002;13:1176–80.
54. Hnatowich DJ, Winnard P, Virzi F, et al. Technetium-99m labeling of DNA oligonucleotides. *J Nucl Med* 1995;36:2306–14. [PubMed: 8523124]

55. Dewanjee MK, Ghafouripour AK, Kapadvanjwala M, et al. Noninvasive imaging of c-myc oncogene messenger RNA with indium-111-antisense probes in a mammary tumor bearing mouse model. *J Nucl Med* 1994;35:1054–63. [PubMed: 8195870]
56. Rao PS, Tian X, Qin W, et al. ^{99m}Tc-peptide nucleic acid probes for imaging oncogene mRNAs in tumors. *Nucl Med Commun* 2003;24(8):857–63. [PubMed: 12869817]
57. Dewanjee MK, Ghafouripour AK, Werner RK, Serafini AN, Sfakianakis GN. Development of sensitive radioiodinated antisense oligonucleotide probes by conjugation technique. *Bioconj Chem* 1991;2:195–200.
58. Smith SV. Molecular imaging with ⁶⁴Cu. *J Inorg Biochem* 2004;98:1874–1901. [PubMed: 15522415]
59. Roivainen A, Tolvanen T, Salomäki S, et al. ⁶⁸Ga-labeled oligonucleotides for in vivo imaging with PET. *J Nucl Med* 2004;45:347–55. [PubMed: 14960659]
60. Tian X, Aruva MR, Zhang K, Cardi CA, Thakur ML, Wickstrom E. PET imaging of *CCND1* mRNA in human MCF7 estrogen receptor-positive breast cancer xenografts with an oncogene-specific [⁶⁴Cu] DO3A-PNA-IGF1 analog radiohybridization probe. *J Nucl Med* 2007;48(10):1699–1707. [PubMed: 17909257]
61. Tian X, Chakrabarti A, Amirkhanov N, et al. Receptor mediated internalization of chelator-PNA-peptide hybridization probes for radioimaging or magnetic resonance imaging of oncogene mRNAs in tumors. *Biochem Soc Trans* 2007;35:72–6. [PubMed: 17233604]
62. Amirkhanov NV, Dimitrov I, Opitz AW, Zhang K, Lackey JP, Cardi CA, et al. Design of (Gd-DO3A)_n-polydiamidopropanoyl-peptide nucleic acid-D (Cys-Ser-Lys-Cys) magnetic resonance contrast agents. *Biopolymers* 2008;89:1061–76. [PubMed: 18680101]
63. Tavitian B. In vivo imaging with oligonucleotides for diagnosis and drug development. *Gut* 2003;52:40–7. [PubMed: 12477757]
64. Lendvai G, Velikyan I, Bergström M, et al. Biodistribution of ⁶⁸Ga-labelled phosphodiester, phosphorothioate and 2'-O-methyl phosphodiester oligonucleotides in normal rats. *Eur J Pharm Sci* 2005;26(1):26–38. [PubMed: 15941654]
65. Roivainen A, Tolvanen T, Salomäki S, et al. ⁶⁸Ga-labelled oligonucleotides for in vivo imaging with PET. *J Nucl Med* 2004;45:347–55. [PubMed: 14960659]
66. Wang J, Chen P, Mrkobrada M, et al. Antisense imaging of epidermal growth factor –induced p21^{WAF-1/CIP-1} gene expression in MDA-MB-468 human breast cancer xenografts. *Eur J Nucl Med* 2003;30:1273–80.
67. Urbain JLC, Shore SK, Vekemans MC, et al. Scintigraphic imaging of oncogenes with antisense probes: does it make sense? *Eur J Nucl Med* 1995;22:499–504. [PubMed: 7556292]
68. Stalteri MA, Mather SJ. Hybridization and cell uptake studies with radiolabeled antisense oligonucleotides. *Nucl Med Commun* 2001;22 (11):1171–79. [PubMed: 11606881]
69. Cammilleri S, Sangrajrang S, Perdereau B, et al. Biodistribution of iodine-125 tyramine transforming growth factor a antisense oligonucleotide in athymic mice with a human mammary tumour xenograft following intratumoral injection. *Eur J Nucl Med* 1996;23:448–52. [PubMed: 8612667]
70. Wickstrom, E.; Thakur, ML.; Sauter, ER. Radiolabeled peptide nucleic acid oncogene probes conjugated to receptor-specific peptide analogs. In: Janson, CG.; During, MJ., editors. *Peptide Nucleic Acids, Morpholinos, and Related Antisense Biomolecules*. New York: Landes Bioscience/Kluwer Academic/Plenum Publishers; 2006. p. 59-86.
71. Tian X, Aruva MR, Qin W, Zhu W, Duffy KT, Sauter ER, Thakur ML, Wickstrom E. External imaging of *CCND1* cancer gene activity in experimental human breast cancer xenografts with [^{99m}Tc] peptide-PNA-peptide chimeras. *J Nucl Med* 2004;45(12):2070–82. [PubMed: 15585484]
72. Tian X, Aruva MR, Qin W, et al. Noninvasive molecular imaging of MYC mRNA expression in human breast cancer xenografts with a [^{99m}Tc] peptide-peptide nucleic acid-peptide chimera. *Bioconj Chem* 2005;16:70–9.
73. Chakrabarti A, Zhang K, Aruva MR, Cardi CA, Opitz AW, Wagner NJ, Thakur ML, Wickstrom E. Radiohybridization PET imaging of *KRAS* G12D mRNA expression in human pancreas cancer xenografts with [⁶⁴Cu] DO3A-peptide nucleic acid-peptide nanoparticles. *Cancer Biology & Therapy* 2007;6(6):948–56. [PubMed: 17611392]

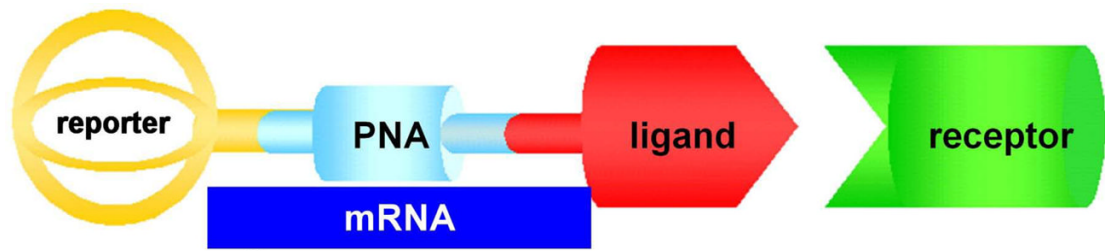


Figure 1. Schematic representation of reporter-PNA-ligand probe wherein reporter can be radioisotope like ^{64}Cu or $^{99\text{m}}\text{Tc}$, or contrast agent like Gd for MRI, bound to macrocyclic chelator DOTA, PNA sequence complementary to oncogene mRNA, and peptide ligand specific for overexpressed receptors on cancer cells.

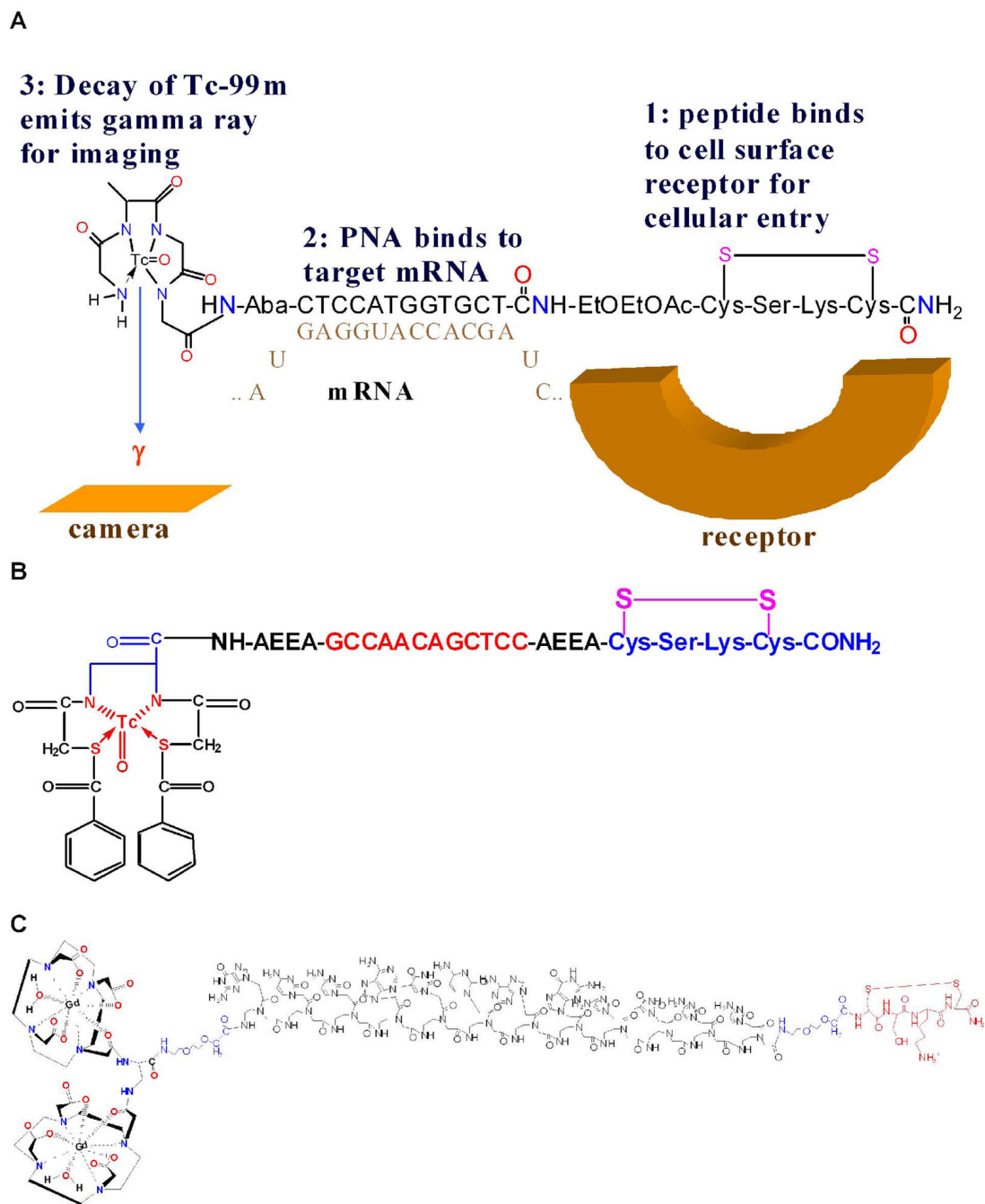


Figure 2.

Radiohybridization and MRI probes

- ^{99m}Tc-PNA-Peptide probe with IGF1 analog specific for IGF1 receptor, PNA sequence complementary to *CCND1* oncogene mRNA, and N₄ chelating peptide GdAGG for chelating ^{99m}Tc for SPECT imaging of breast cancer.
- SBTG2-KRAS PNA-Peptide probe with IGF1 analog specific for IGF1 receptor, PNA sequence complementary to *KRAS* D12 mutant, and N₂S₂ chelator for ^{99m}Tc or ⁶⁴Cu for SPECT or PET imaging of pancreatic cancer.
- MRI probe with IGF1 analog specific for IGF1 receptor, PNA sequence complementary to *KRAS* D12 mutant, and DOTA for chelating Gd for MRI of pancreatic cancer.

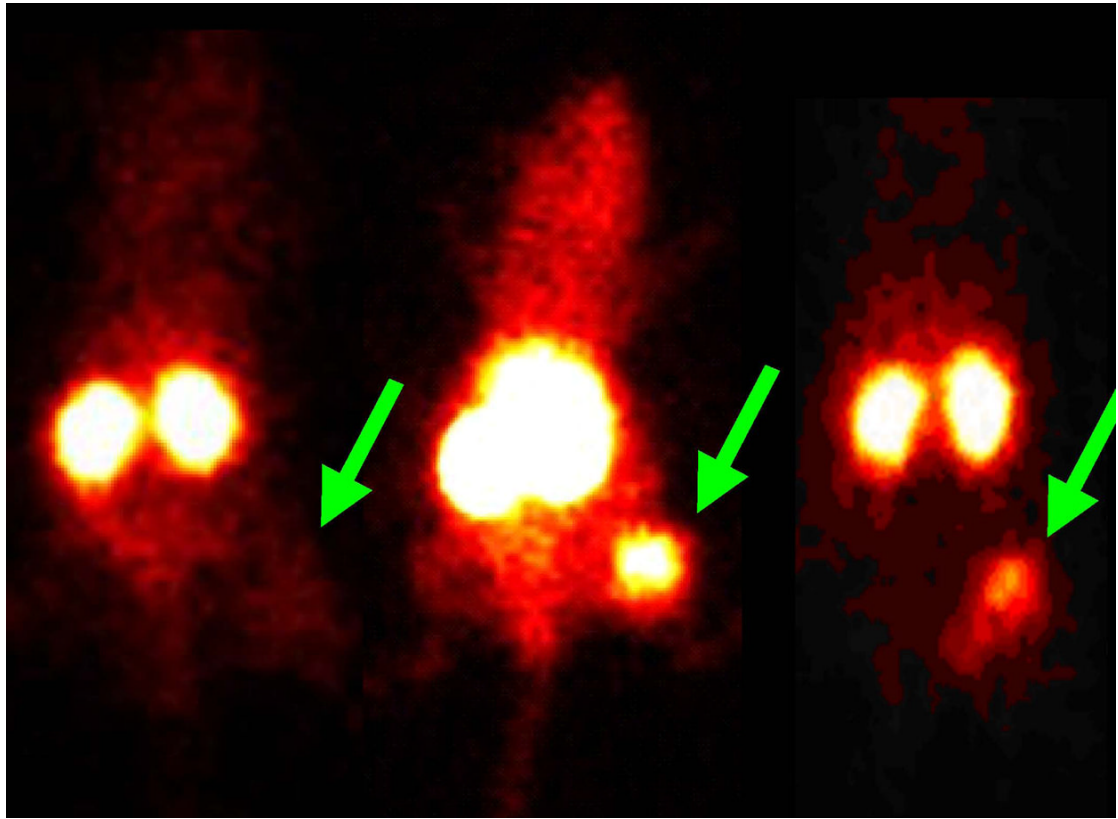


Figure 3. Scintigraphic images in nude mice bearing human MCF-7 breast tumor xenograft at 4, 12 and 24 h p.i. of ^{99m}Tc -*CCND1* PNA-peptide probe. (Reprinted, with permission, from reference 67).

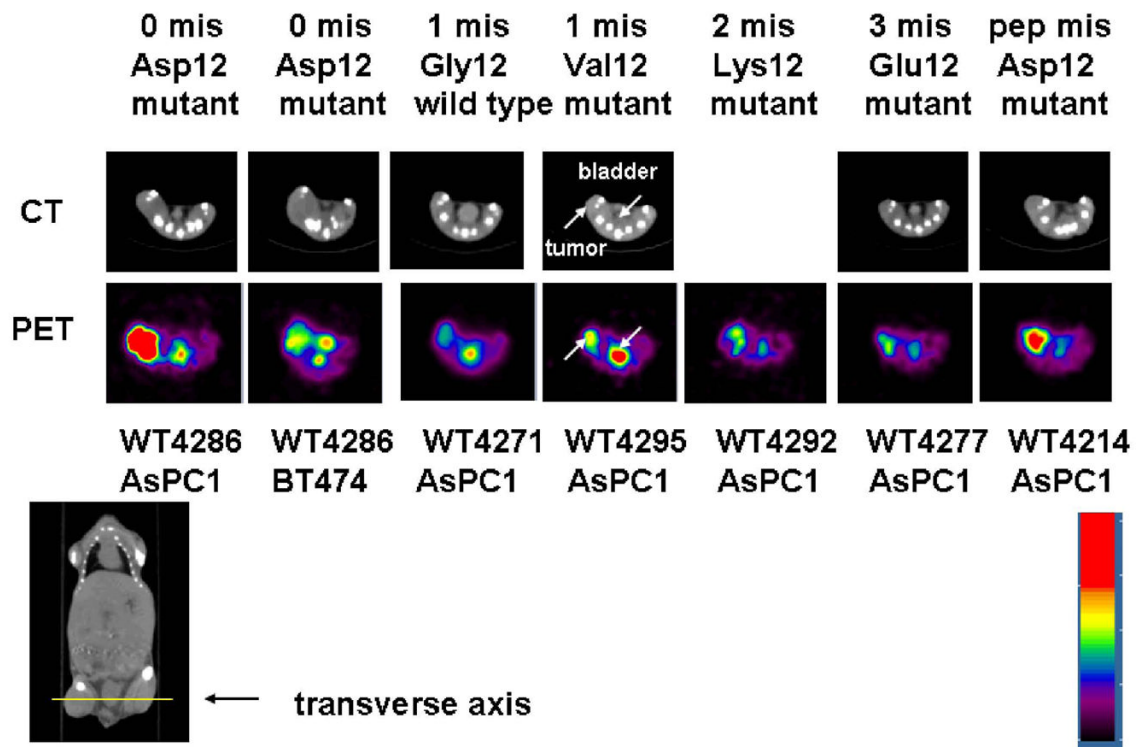


Figure 4.

Transverse CT images (top row) and PET images (second row) of ^{64}Cu *KRAS* D12PNA peptide probe WT4286 vs. 1 mismatch WT4271, 1-mismatch WT4295, 2-mismatch WT4292, 3 mismatch WT4277 and a peptide mismatch WT4214 in human ASPC1 pancreatic xenografts in immunocompromised mice 24 h after probe administration into the tail vein. The mouse second from left bears human BT474 breast cancer xenograft lacking activated *KRAS*. The yellow line on the coronal CT image shows the level of the transverse images. The color scale of the images was normalized to the max/min of frame to show the dynamic range of tumor uptake. (Reprinted, with permission, from reference 69).

Table 1

Key components in development of antisense imaging agents

Stage and goals	Test system	Approaches and requirements
I. Design of oligonucleotides		<ul style="list-style-type: none"> Based on Watson-Crick base pairing and computer aided target selection. Selection of modifications/suitable chemistry for synthesis to achieve <i>in vivo</i> stability and desired pharmacokinetics. Optimization to achieve high yield and purity. Conjugation of chelating groups and moieties to the sequence for radiolabeling and for achieving cell specific uptake. Design of mismatch sequences to serve as controls.
II. Target validation: Specificity and efficiency	Cell free system	<ul style="list-style-type: none"> Estimation of T_m to demonstrate specificity.
III. Radiolabeling		<ul style="list-style-type: none"> Optimization of radiolabeling. Characterization and purification of radiolabeled antisense probe.
IV. <i>In vitro</i> biological activity: Specificity and efficiency	Cell culture	<ul style="list-style-type: none"> Studies to demonstrate kinetics of uptake and efflux in cells expressing target mRNA. Studies to evaluate S1 nuclease protection of target mRNAs by antisense probe. Uptake and hybridization of radiolabeled probe to the target sequence by northern analysis.
V <i>In vivo</i> pharmacokinetics	Animal models	<ul style="list-style-type: none"> Determination of pharmacokinetics of the probe, target to nontarget ratios by tissue distribution and imaging studies. Studies to demonstrate specific uptake in the target tissue and hybridization of the probes to the target sequence. Estimation of mRNA expression in the target tissue by conventional methods like RT-PCR and comparison with uptake of radiolabeled antisense agent.
VI. <i>In vivo</i> toxicology	Animal	<ul style="list-style-type: none"> Determination of toxicity due to radionuclides if any, or due to antisense sequences.
VII. Large scale synthesis and radiolabeling		<ul style="list-style-type: none"> Synthesis and radiolabeling complying good manufacture practice (GMP).
VIII. Clinical evaluation and regulatory issues	Humans	<ul style="list-style-type: none"> Phase I to IV trials

Table 2

Sequence of PNA probes

Name	Sequence
PNA-free (WT990)	Gly-D-Ala-Gly-Gly-Aba- (Gly) ₄ -D (Cys-Ser-Lys-Cys)
MYCC	
<i>MYCC</i> PNA antisense (WT4219)	Gly-D-Ala-Gly-Gly-Aba-GCATCGTCGCGG-AEEA-D (Cys-Ser-Lys-Cys)
<i>MYCC</i> PNA mismatch (WT4235)	Gly-D-Ala-Gly-Gly-Aba-GCATGTCTGCGG-AEEA-D (Cys-Ser-Lys-Cys)
CCND1	
<i>CCND1</i> PNA antisense (WT4185)	Gly-D-Ala-Gly-Gly-Aba-CTGGTGTTCCAT-AEEA-D (Cys-Ser-Lys-Cys)
<i>CCND1</i> PNA mismatch (WT4172)	Gly-D-Ala-Gly-Gly-Aba-CTGGACAACCAT-AEEA-D (Cys-Ser-Lys-Cys)
<i>CCND1</i> peptide mismatch (WT4113)	Gly-D-Ala-Gly-Gly-Aba-CTGGTGTTCCAT-AEEA-D (Cys-Ala-Ala-Cys)
Fl- <i>CCND1</i> PNA antisense (WT4433)	SFX-AEEA-CTGGTGTTCCAT-AEEA-D (Cys-Ser-Lys-Cys)
Fl- <i>CCND1</i> peptide mismatch (WT4361)	SFX-AEEA-CTGGTGTTCCAT-AEEA-D (Cys-Ala-Ala-Cys)
KRAS	
<i>KRAS</i> PNA antisense	SBTG ₂ -DAP-AEEA-GCCAACAGCTCC-AEEA-D (Cys-Ser-Lys-Cys)
<i>KRAS</i> PNA antisense (WT4286, Asp 12 mutant)	DOTA-AEEA-GCCATCAGCTCC-AEEA-D (Cys-Ser-Lys-Cys)
<i>KRAS</i> PNA, 1 mismatch (WT4271, Gly12 wild type)	DOTA-AEEA-GCCACAGCTCC-AEEA-D (Cys-Ser-Lys-Cys)
<i>KRAS</i> PNA, 1 mismatch (WT4295, Val12 mutant)	DOTA-AEEA-GCCACAGCTCC-AEEA-D (Cys-Ser-Lys-Cys)
<i>KRAS</i> PNA, 2 mismatch (WT4292, Lys 12 mutant)	DOTA-AEEA-GCCTAGCTCC-AEEA-D (Cys-Ser-Lys-Cys)
<i>KRAS</i> PNA, 3 mismatch (WT4277, Glu12 mutant)	DOTA-AEEA-GCCTTTGCACC-AEEA-D (Cys-Ser-Lys-Cys)
<i>KRAS</i> PNA antisense, peptide mismatch (WT4214, Asp12 mutant)	DOTA-AEEA-GCCATCAGCTCC-AEEA-D (Cys-Ala-Ala-Cys)
Fl= Fluoresceinyl; SFX= 6-(fluorescein-5-carboxamido) hexanoyl	